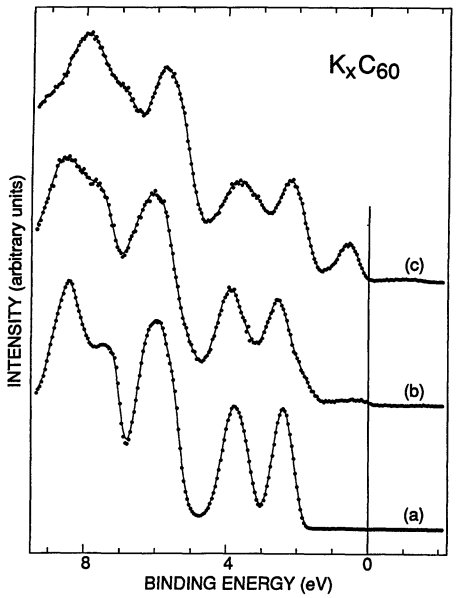

Fig. 3. Valence-band photoemission spectra of K_xC_{60} films prepared by vacuum doping, compared to that of C_{60}. The zero of the energy scale is at the Fermi level of the spectrometer, determined from the Fermi cutoff in In.

sition to the bcc (body-centered-cubic) structure, which can accommodate six interstitials per molecular C_{60} unit.

The apparent similarity between the reaction of C_{60} with K and the formation of graphite intercalation compounds is, at first sight, surprising. Graphite is a semimetal with strongly dispersing π bands that overlap at the Fermi energy. Solid C_{60} is a molecular insulator with narrow bands and a gap of 1.9 eV between the HOMO and LUMO. Nevertheless, there is no doubt that in both materials a metal results from the donation of alkali conduction electrons into unoccupied states of the native material. However, it appears that in solid C_{60} the charge transfer is nearly complete, that is, one electron is transferred per intercalated K atom. In graphite intercalation compounds the charge transfer inferred from measurements of photoemission intensity near the Fermi energy is less than unity, with a value of 0.3 obtained for Cs (*10*). However, band mapping of LiC_6 shows that the Li 2*s* band lies above the Fermi level and that the rigid band model is not obeyed (*11*).

REFERENCES

1. W. Krätschmer, L. D. Lamb, K. Fostiropoulos, D. R. Huffman, *Nature* **347**, 354 (1900).
2. D. L. Lichtenburger, K. W. Nebesny, C. D. Ray, D. R. Huffman, L. D. Lamb, *Chem. Phys. Lett.* **176**, 203 (1991).
3. J. H. Weaver *et al.*, *Phys. Rev. Lett.* **66**, 1741 (1991).
4. R. C. Haddon *et al.*, *Nature* **350**, 320 (1991).
5. A. F. Hebard *et al.*, *ibid.*, p. 600.
6. R. M. Fleming *et al.*, *Mater. Res. Soc. Symp. Proc.* **206**, in press.
7. D. M. Riffe, G. K. Wertheim, P. H. Citrin, *Phys. Rev. Lett.* **64**, 571 (1990).
8. R. C. Haddon, L. E. Brus, K. Raghavachari, *Chem. Phys. Lett.* **125**, 459 (1986).
9. A. F. Wells, *Structural Inorganic Chemistry* (Clarendon Press, Oxford, ed. 5, 1986), p. 422.
10. P. Oelhafen, P. Pfluger, E. Hauser, H.-J. Güntherodt, *Phys. Rev. Lett.* **44**, 197 (1980).
11. W. Eberhardt, I. T. McGovern, E. W. Plummer, J. E. Fischer, *ibid.*, p. 200.

22 April 1991; accepted 15 May 1991

Molecular Beam Scattering from Liquid Surfaces

MARY E. SAECKER, STEVEN T. GOVONI, DANIEL V. KOWALSKI, MACKENZIE E. KING, GILBERT M. NATHANSON*

By means of controlled collisions of atoms and molecules with liquid surfaces, molecular beam experiments can be used to probe how gases stick to, rebound from, and exchange energy with molecules in the liquid phase. This report describes measurements of energy exchange in collisions between gases (neon, xenon, and sulfur hexafluoride) and polyatomic liquids (squalane and perfluoropolyether). Energy transfer depends critically on liquid composition and is more efficient for the hydrocarbon than for the perfluorinated ether.

COLLISIONS BETWEEN GAS-PHASE and liquid-phase molecules are the first step in establishing mechanical, thermal, and chemical equilibrium between gases and liquids. Gas-phase molecules striking a liquid can scatter immediately away or they can bind to liquid-phase molecules at the surface on their way to solvation, reaction, film formation, or evaporation. These elementary processes can be probed by molecular beam scattering techniques that are widely applied to gas-gas and gas-solid chemical reactions (*1*). By directing beams of atoms and molecules at liquids of low vapor pressure in vacuum, we are learning how gases stick to, rebound from, and exchange energy with organic and inorganic liquids. Scattering experiments on liquids have been performed only rarely (*2*). We describe here studies to measure the exchange of energy when gases (Ne, Xe, and SF_6) collide with polyatomic liquids (perfluoropolyethers and hydrocarbons). Our experiments show that the amount of energy transferred on impact depends critically on the nature of the liquid.

We used two liquids: squalane, a long-chain hydrocarbon, and Krytox 1506, a long-chain perfluorinated polyether (PFPE). Squalane (99.9%, Aldrich), 2,6,10,15,19,23-hexamethyltetracosane, has a density of 0.81 g/cm^3, a vapor pressure below 10^{-7} torr, a surface tension of 30 dyne/cm, and a viscosity of 0.3 poise at 25°C. Krytox 1506 (Du Pont), $F\text{-}[CF(CF_3)CF_2O]_{14(avg)}\text{-}CF_2CF_3$, has a density of 1.88 g/cm^3. Its vapor pressure lies below 4×10^{-7} torr, and it has a surface tension of 18 dyne/cm and a viscosity of 1.3 poise.

The liquids are placed inside a high-vacuum chamber to remove ambient gases and to allow the incident beam of atoms or molecules to collide only with the liquid surface. Impinging beams are created by expanding Ne, Xe, or SF_6 mixed with He or H_2 through a pinhole aperture at 295 K. The nearly monoenergetic beam strikes the liquid surface, and the recoiling species are monitored by a mass spectrometer oriented at 90° to the incident beam. The raw data are time-of-flight (TOF) spectra that record the time for the scattered species to travel 19.5 cm from a slotted wheel to the mass spectrometer. The spinning wheel chops the scattered beam into 11- or 28-μs pulses to measure arrival times. In these studies, the liquid surface is oriented at 45° with respect to both the incident beam and the mass spectrometer; the peak arrival times, however, do not change with surface rotation.

Clean and continuously renewed liquid surfaces are produced by two methods shown in Fig. 1. In one method (Fig. 1A), a vertical, ribbon-like stream is produced by liquid flowing through a highly polished stainless steel jet with a rectangular exit slit 5.0 mm by 0.3 mm (*3*). The incident beam strikes the planar liquid surface (moving at 100 cm/s) as it leaves the jet. The stream is then recirculated by a vacuum-sealed gear pump. A second method (Fig. 1B) uses a slowly rotating wheel that is partially immersed in a liquid reservoir (*4*). The wheel drags along a thin liquid film that is scraped by a razor blade, leaving behind a liquid layer 0.25 mm deep. The molecular beam strikes the freshly wiped surface 0.25 s later. Laser reflections from the fresh surface show that it is macroscopically flat to within 0.5°. The data presented here were recorded with

Department of Chemistry, University of Wisconsin–Madison, Madison, WI 53706.

*To whom correspondence should be addressed.

this second method, but in direct comparisons the jet and wheel techniques generated identical TOF spectra.

Each liquid was thoroughly degassed before the reservoir was filled. Pump oils and finger grease do not spread on either liquid; because of the low surface tensions of the liquids, bulk contaminants will not preferentially collect at the surface. The liquids were not contaminated during the experiments (the surface tensions differed by less than 0.1 dyne/cm before and after each run).

The TOF spectra in Figs. 2, 3, and 4 show how high-velocity Ne and Xe atoms and SF_6 molecules scatter from liquid-phase PFPE and squalane. The Ne, Xe, and SF_6 flight times are very different for squalane and PFPE. For many encounters the gases do not stick and evaporate thermally but instead fly away from the surface at velocities determined by the liquid's response to the transient collision.

Figure 2, A and B, shows TOF spectra of Ne atoms scattering from PFPE and squalane, respectively, after impact at a collision energy E_c of 25 kJ/mol, five times the average translational energy of Ne atoms at room temperature. The peak arrival times of 155 μs for Ne/squalane and 125 μs for Ne/PFPE are much shorter than the 275-μs flight time for thermal evaporation of Ne at the surface temperature of 295 K; the Ne atoms recoil at high, nonthermal velocities from both liquids.

We can analyze these spectra further by determining the kinetic energies of the scattered Ne atoms from their arrival times (Fig. 2, C and D). The solid translational energy curves yield the solid line fits to the TOF spectra. There is a broad distribution of recoil energies when Ne strikes squalane, whereas two distinct channels are apparent for Ne/PFPE. The energy lost by a Ne atom on impact is deposited into the hindered vibrational, torsional, and translational motions of the liquid-phase molecules. This energy transfer is equal to the difference between the incident and final Ne translational energies.

We can interpret the translational energy data by appealing to two limiting processes that frequently occur in gas-solid collisions: direct inelastic scattering (IS) and trapping desorption (TD) (*5, 6*). The dashed lines in Fig. 2 illustrate the decomposition of the overall curves into these two processes. Inelastically scattered gases transfer only a fraction of their energy to the liquid-phase molecules during the transient collision. They recoil with high translational energies and arrive at early times at the mass spectrometer. In contrast, molecules that collide multiple times transfer energy very efficiently and are momentarily trapped by the liquid. They desorb at velocities characteristic of thermal evaporation and arrive at the mass spectrometer at long times (*5, 6*). Low incident energy SF_6 (E_c = 11 kJ/mol) and Xe (E_c = 6 kJ/mol) desorb thermally after colliding with squalane and nearly thermally from PFPE. At high impact energies, however, most Ne, Xe, and SF_6 scatter inelastically from the surface while a smaller number exit at much lower velocities. This slower TD component mimics a thermal distribution but lacks the slowest species that would be present in a Boltzmann distribution at 295 K. We determined the inelastic component by subtracting this nearly thermal distribution from the solid translational energy curve.

We estimate from the dashed line fits of Fig. 2 that 85% of the Ne atoms scatter inelastically from PFPE, while roughly 75% do so from squalane. In these inelastic channels, Ne scatters from PFPE with an average translational energy of 19 kJ/mol, corresponding to a transfer of roughly 25% of the impact energy to the liquid, whereas squalane absorbs on average 36% of the collision energy. Although only a fraction of

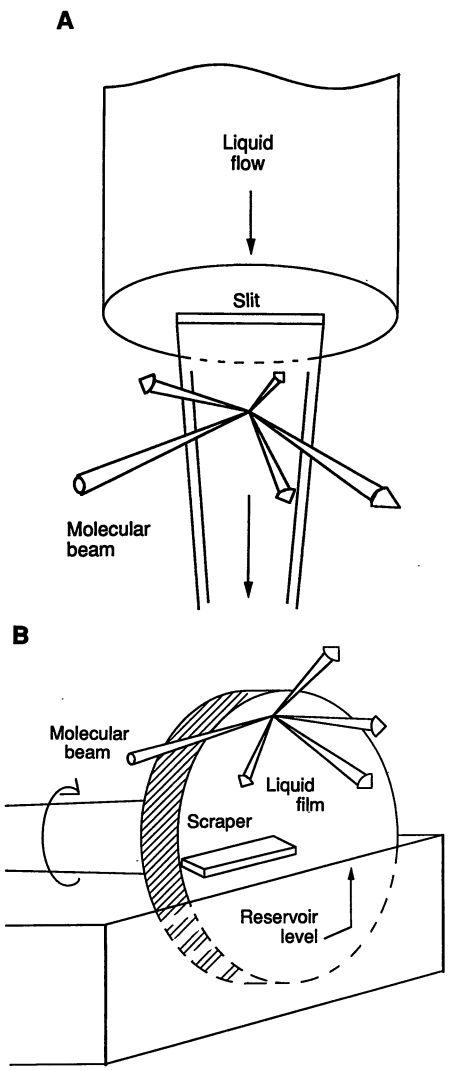

Fig. 1. Illustration of a beam of molecules colliding with (**A**) a vertical liquid ribbon produced by a planar jet and (**B**) a liquid film dragged by a rotating wheel.

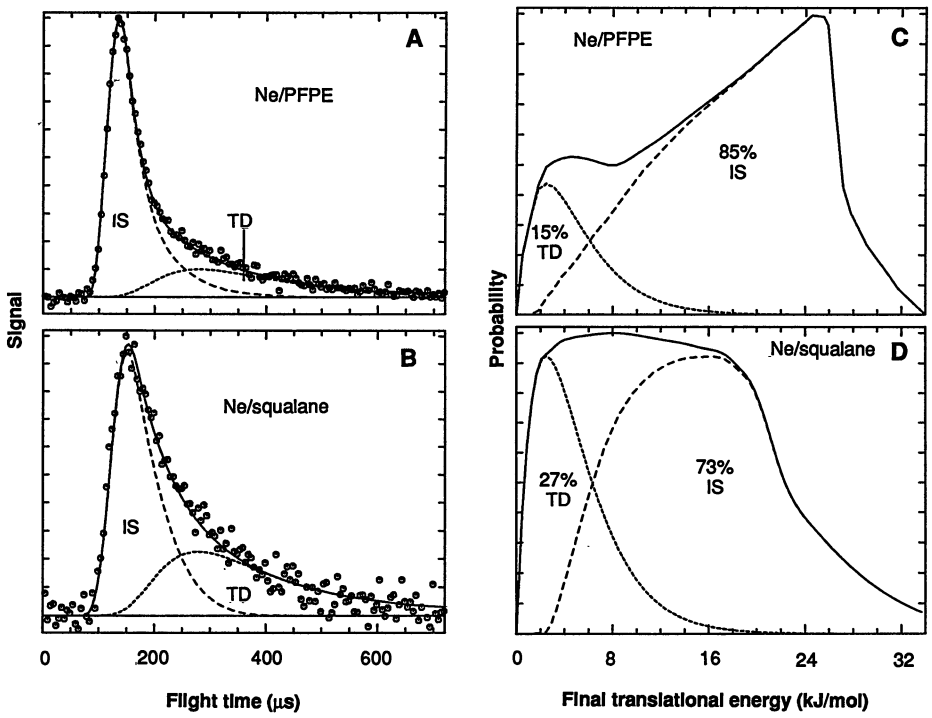

Fig. 2. TOF spectra of Ne atoms scattering from (**A**) PFPE and (**B**) squalane after impact at a collision energy E_c of 25 kJ/mol. Ion flight times and electronic delays have been subtracted from the spectra. (**C** and **D**) Translational energy distributions of the scattered Ne atoms. The solid curves are derived from the TOF spectra. IS, inelastic scattering component under the dashed line; TD, trapping desorption component under the dotted line.

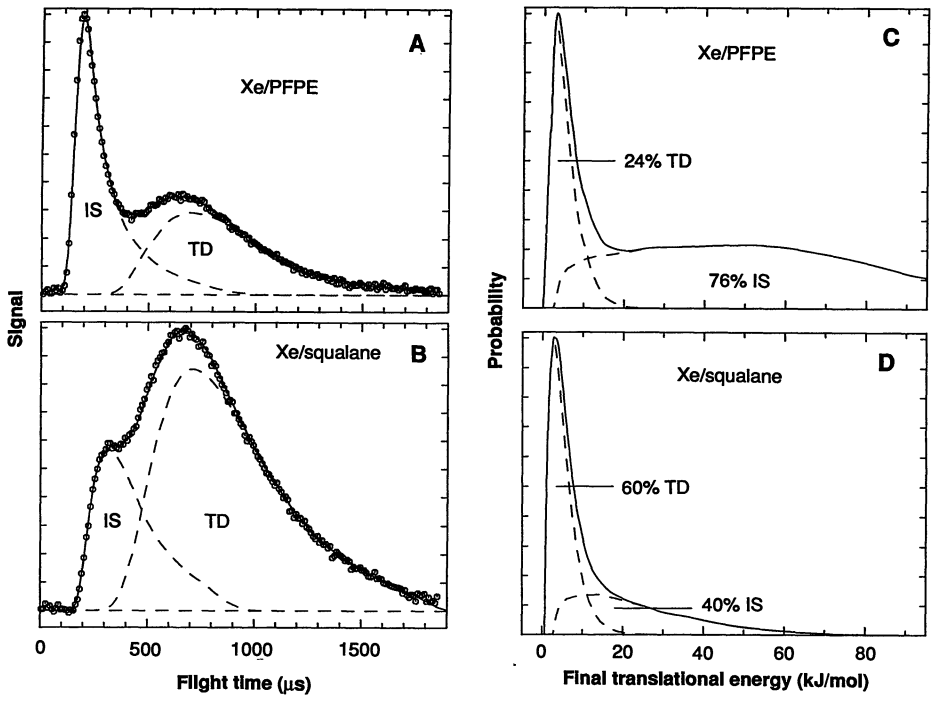

Fig. 3. (**A** and **B**) TOF spectra; (**C** and **D**) translational energy distributions for Xe scattering from PFPE and squalane. E_c = 220 kJ/mol.

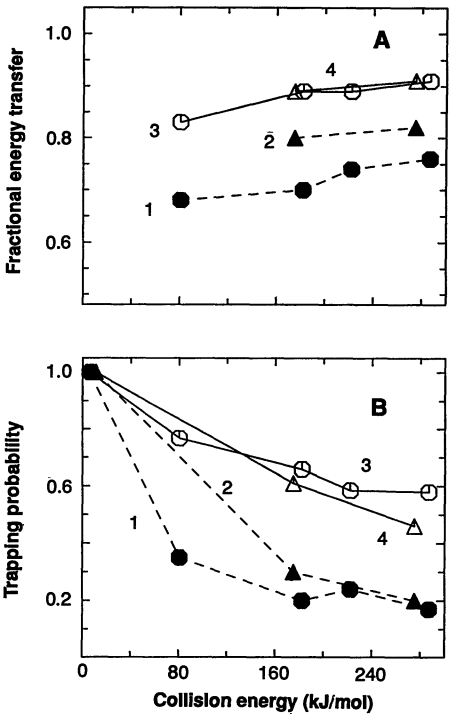

Fig. 5. (**A**) Gas to liquid energy transfer for IS and (**B**) fraction of collisions leading to TD. Curve 1, Xe/PFPE; curve 2, SF_6/PFPE; curve 3, Xe/squalane; and curve 4, SF_6/squalane.

the Ne atoms reflect from these surfaces without energy loss, both the hydrocarbon and fluorocarbon liquids channel most of the initial impact back into Ne translational motion. Collision energies of 25 kJ/mol greatly exceed Ne-liquid binding energies, and neither liquid efficiently accommodates the impinging atom through trapping or solvation. Even at E_c = 6 kJ/mol, Ne does not completely equilibrate upon collision.

These Ne scattering results differ remarkably from collisions of heavy species with squalane or PFPE. Figure 3 shows how Xe atoms interact with each liquid at E_c = 220 kJ/mol. Squalane and PFPE respond in strikingly different ways; each TOF spectrum consists of two peaks, but the fast, high energy spike dominates only when Xe collides with PFPE. We attribute the slower signal to Xe TD and the sharp peaks to IS. For squalane, Xe recoils promptly in 40% of the collisions, losing on average 90% of its energy on impact. In contrast, almost twice as many Xe atoms scatter inelastically from PFPE and they retain over 25% of their collision energy. These two peaked spectra persist at least down to E_c = 80 kJ/mol.

We can also ask what happens when Xe is replaced by SF_6, a polyatomic molecule of nearly equal size and mass. SF_6 scattering mimics the Xe data closely (Fig. 4), even though SF_6 has fifteen vibrational and three rotational modes. Energy transfer and trapping probabilities for Xe and SF_6 collisions with squalane and PFPE are displayed in Fig. 5. This figure shows that Xe (circles) and SF_6 (triangles) scatter with similar kinetic energies and trapping probabilities from the hydrocarbon (open symbols), although Xe suffers less energy loss to PFPE (filled symbols) than does SF_6. At high impact energies squalane is much more efficient than PFPE at trapping heavy atoms and molecules and stealing energy away from those that scatter inelastically (Fig. 5).

The startling differences between squalane and PFPE can be interpreted by assuming a billiard ball–like collision between the gas-phase atom and liquid-phase molecules. In the simplest picture, the gas atom of mass m_g collides with surface atoms that belong to one or several molecules and that respond collectively as a single particle of mass m_s struck in an isolated, binary collision (*7, 8*). The fraction of energy transferred to the liquid depends only on the ratio m_g/m_s and not on the collision energy. The data in Fig. 5A show little variation with incident energy, in rough accord with this prediction. The model also predicts that the fraction of energy transferred on impact increases as the effective surface mass m_s decreases. We estimate from the measured energy loss for Xe collisions that the effective mass of squalane lies near 250 atomic mass units (amu) or the equivalent of 60% of a squalane molecule (*9*). The smaller energy transfer to PFPE implies a larger effective mass (430 amu), corresponding to about 2.5 monomer units. In this model, the more efficient energy transfer to squalane correlates with its lighter hydrocarbon structure in comparison with the heavier fluorocarbon structure of PFPE (*8*).

The differences in heavy particle scattering from the hydrocarbon and perfluorinated liquids are easily discernible without detailed analysis. Similar distinctions may apply to other molecular structures. This would provide a possible means of identifying which functional groups of polyatomic molecules protrude at the liquid surface.

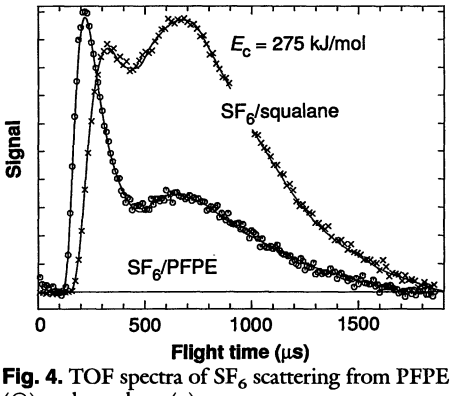

Fig. 4. TOF spectra of SF_6 scattering from PFPE (○) and squalane (x).

REFERENCES AND NOTES

1. Y. T. Lee, *Science* **236**, 793 (1987); S. T. Ceyer, *ibid.* **249**, 133 (1990).
2. M. Sinha and J. B. Fenn, *Proc. 5th Int. Symp. Mol. Beams* (1975). Related evaporation studies include M. Faubel and Th. Kisters [*Nature* **339**, 527 (1989)]; D. R. Olander, M. Balooch, and W. Siekhaus [*J. Phys. Chem.* **90**, 4397 (1986)]; and (*4*).
3. Radiant Dyes Chemie model RDSN06.
4. S. A. Lednovitch and J. B. Fenn, *Am. Inst. Chem. Eng. J.* **23**, 454 (1977).
5. J. E. Hurst *et al.*, *Phys. Rev. Lett.* **43**, 1175 (1979).

6. C. T. Rettner, E. K. Schweizer, C. B. Mullins, *J. Chem. Phys.* **90**, 3800 (1989).
7. A. Amirav, M. J. Cardillo, P. L. Trevor, C. Lim, J. C. Tully, *ibid.* **87**, 1796 (1987).
8. S. Cohen, R. Naaman, J. Sagiv, *Phys. Rev. Lett.* **58**, 1208 (1987).
9. As in (*8*), we calculate the surface mass using the total incident velocity.
10. This work was supported by Dreyfus and Du Pont Young Faculty awards, the National Science Foundation (NSF), the Petroleum Research Fund of the American Chemical Society, and the University of Wisconsin. M.E.S. is supported by NSF and Kodak predoctoral fellowships. G.M.N. is an NSF Presidential Young Investigator.

14 January 1991; accepted 4 April 1991

Programmed Cell Death of T Cells Signaled by the T Cell Receptor and the α_3 Domain of Class I MHC

SURYAPRAKASH R. SAMBHARA AND RICHARD G. MILLER*

As well as being activated or rendered unresponsive, mature T lymphocytes can be deleted, depending on the signals received by the cell. Deletion by programmed cell death (apoptosis) is triggered if a T cell that has received a signal through its T cell receptor complex also receives a signal through the α_3 domain of its class I major histocompatibility complex (MHC) molecule. Such a signal can be delivered by a CD8 molecule, which recognizes the α_3 domain, or by an antibody to this domain. Precursors of both cytotoxic T lymphocytes (CTL's) and T helper cells are sensitive to this signal but become resistant at some point before completing differentiation into functioning CTL's or T helper cells. Because CTL's carry CD8, they can induce cell death in T cells that recognize them. This pathway may be important in both removal of autoreactive T cells and immunoregulation.

ACTIVATION OF A T LYMPHOCYTE requires occupancy of its antigen-specific cell surface receptor (TcR) by its appropriate ligand (processed antigen presented by class I or class II MHC molecules) and a second signal from a growth factor. If the second signal is not provided, the T cell becomes unresponsive (anergic) (*1*). We now present evidence for a pathway that leads to death of T lymphocytes that have been signaled through their TcR and then also receive a signal through the α_3 domain of their class I MHC molecule.

Short-term tissue culture studies of mouse lymphocytes in the mixed lymphocyte reaction (MLR) (*2*) have shown that CTL's can inactivate CTL precursors (CTLp's) that recognize them. This process does not involve the receptor of the CTL being recognized and can occur in the presence of cells and factors that can produce activation (*3*). This implies that, on being recognized, CTL's deliver a signal leading to inactivation; that is, they are acting as specialized antigen presenting cells (veto cells) (*4*) that inactivate T cells that recognize them. CTL's reactive to class I MHC (the majority) also carry the cell surface molecule CD8, which can recognize the α_3 domain of class I MHC (*5*). This binding can strengthen the adhesion of a CTL or CTLp to a cell it recognizes by binding to class I MHC molecules on that cell, thus facilitating T cell responses. We test here whether the CD8 molecule has a second function: Can a CD8 molecule on a cell being recognized by a T cell trigger the inactivation of that T cell by interacting with its class I MHC?

Paired $CD8^+$ and $CD8^-$ CTL lines of mouse origin were derived from two independent MLR with F_1(BALB/c × RNC) as responders and C57BL/6 (B6) as stimulators (*6*). All four lines had an αβ TcR, similar specificity (anti-D^b), and similar cytotoxic activity. The $CD8^+$ lines ($H\text{-}2^{d/k}$), when added to an MLR, reduced development of cytotoxic activity when BALB/c ($H\text{-}2^d$) were used as stimulators (MHC was shared with the added CTL's), but had no effect when SWR ($H\text{-}2^q$) were used as stimulators (no MHC sharing) (Fig. 1A). The $CD8^-$ CTL line had no effect on the response in either MLR.

We reasoned that covering the CD8 molecule on a $CD8^+$ CTL with a monoclonal antibody (MAb) to CD8 should block its ability to inactivate CTLp's. However, a MAb to CD8 would also block response induction (*7*). We therefore used a MAb specific for one of the two allelic forms of the mouse CD8 molecule (Ly-2.1 and Ly-2.2). MLR's were set up in which both responders (SJL and $H\text{-}2^s$) and stimulators (BALB/c and $H\text{-}2^d$) were Ly-2.2. To these were added CTL's from either BALB/c (identical to stimulator) or DBA/2 (same MHC but Ly-2.1) in the presence or absence of MAb to Ly-2.1. Both CTL lines produced equivalent response reduction in the absence of added MAb to Ly-2.1 but, as predicted, the response reduction produced by the Ly-2.1^+ DBA/2 CTL line was partly reversed by addition of the MAb to Ly-2.1 (Fig. 1B).

These results suggested that any cell line might inactivate CTLp's recognizing it if it were transfected with CD8. We compared the ability of a TcR^- $CD4^-$ $CD8^-$ BW 5147 T lymphoma line ($H\text{-}2^k$) to inactivate CTLp's reactive against $H\text{-}2^k$ with that of cells from the same line transfected with either CD8 (*8*) or CD4 (*9*). Appropriate expression of CD4, CD8, and $H\text{-}2^k$ was confirmed by flow cytometry (*10*). Only the $CD8^+$ lymphoma produced inhibition of the anti-$H\text{-}2^k$ MLR (Fig. 1C). This experiment provides direct evidence for the role of CD8 in the inactivation of CTLp's and also demonstrates that cells do not need to have the cytotoxic machinery of a CTL or to carry a TcR to be able to produce inactivation of CTLp's.

The MAb 34-2-12S (*11*), referred to as anti-α3, is known to bind to the α_3 domain of H-2 class I D^d MHC molecules (*12*). In that CD8 also binds to the α_3 domain, addition of this MAb to an MLR in which the responder cells carried D^d might mimic the effect of adding cells expressing CD8. The effects of adding anti-α_3 or control MAb on cell number, CTL activity, and interleukin-2 (IL-2) production in an MLR containing D^d-bearing responder cells were determined (experiment 1, Table 1). The control MAb's, of the same isotype (IgG2a) and generated in the same immunization protocol (*11*), all interact with class I MHC but appear not to interact with the α_3 domain (*12*). Anti-α3 prevented development of cytotoxic activity whereas the other MAb's to MHC had no effect (*13*). Surprisingly, both total cell number and IL-2 production [a measure of T helper cell (Th) activity] were also greatly reduced by anti-α3 but not by the other MAb's. One interpretation is that T helper precursors (Thp's), as well as CTLp's, are inactivated if they also receive a signal through the α_3 domain of their class I MHC molecule.

MAb 28-14-8S (*14*) is a second MAb known to bind to a class I MHC α_3 domain, in this case D^b (*15*). It also produced reduction of both cytotoxic activity and IL-2 production whereas control MAb's (*14, 15*) did not (experiment 2, Table 1A) (*16*).

The inactivation of CTLp's produced by added CTL's occurs early in an MLR; added CTL's have little or no effect if added later than 2 days after initiation (*3*). Similarly,

Ontario Cancer Institute and Department of Immunology, University of Toronto, 500 Sherbourne Street, Toronto, Ontario, Canada, M4X 1K9.

*To whom correspondence should be addressed.